Analyst

PAPER

View Article Online
View Journal

Cite this: DOI: 10.1039/c9an00555b

Improvement of biosensor accuracy using an interference index detection system to minimize the interference effects caused by icterus and hemolysis in blood samples†

Sungha Park

Received 27th March 2019,
Accepted 22nd July 2019

DOI: 10.1039/c9an00555b

rsc.li/analyst

Reagent sensors in diagnostic assays are used in medical laboratories to obtain patient results. However, interference during the analysis of blood samples is a constant problem with reagent sensors and leads to inaccurate results. Interference in blood analysis is frequently caused by hemolysis and icterus. This study analyzed the effects of interferents on reagent sensors and devised a method to improve the measurement accuracy using an interference index detection (IID) system to minimize the interference effect. The IID system can be easily applied using only two wells and an optical component for sample measurement. After applying the IID system, the interference rates from bilirubin and hemoglobin improved dramatically. A comparison of results obtained for clinical samples showed that the IID system had a positive effect on the accuracy.

1 Introduction

In vitro diagnostic (IVD) medical devices containing reagent sensors are used to perform tests on human blood samples. The results are used to diagnose medical conditions, help detect infection, and monitor drug therapies in clinical laboratories. Although IVDs play an important role in the diagnosis and treatment of patient disease, interference can affect the reactions used to detect the target substance and may lead to false positives. Interference can increase the error in the results and reduce the diagnostic accuracy. Particularly with the blood analyzers used by doctors and clinical pathologists, interference tests are conducted using bilirubin and hemoglobin, which are produced by icterus and hemolysis, and the results are used as important performance indicators and clinical guides. Interference is a constant problem when analyzing blood using IVDs in clinical laboratories.[1]

Interference from icterus and hemolysis can occur during the blood handling or collection processes, or result from the color/turbidity of the blood itself.[2,3] Hemolysis occurs when hemoglobin is released into the blood plasma on specimen collection when blood is shaken too vigorously or is centrifuged before coagulation is complete, during freeze–thaw cycles of whole blood, or when blood is collected through an intravenous cannula.[4–6] Icterus affects spectral absorption because bilirubin is yellow.[7,8] Because the compounds icterus and hemolysis produce have optical effects, they negatively affect IVD devices that measures reagent reactions using spectrophotometry. This interference affects assays that use color detection for diagnosis, such as those that test for different clinical chemistry, electrolytes.[9]

Traditionally, sample pretreatment is used to remove interference.[10] However, this requires additional experimental procedures that can affect the sample usability and measurement time, and the accuracy improvement is limited. Consequently, various manufacturers are investigating procedures for using an interference index with IVD devicess.[2,11,12] However, this is not an ideal solution because it can only be utilized as a guide of target analysis results through interference index provision. It is important to improve interference effects and provide more accurate measurements for diagnosis when measuring samples containing an interferent under harsh conditions.

In this paper, the interference effects of bioassay sensors were analyzed and a method was devised to improve the measurement accuracy by minimizing the interference effect using the optical characteristics of icterus and hemolysis in blood samples.

2 Materials and methods

2.1 Materials

Poly(vinyl chloride), bis(2-ethylhexyl)sebacate, tris(2-ethylhexyl) phosphate, trioctyltin chloride, chromoionophore VI, cyclohexanone, hemoglobin, and bilirubin were purchased from Sigma-Aldrich (St Louis, MO, US). Bicine, 2-(*N*-morpholino)

IVD R&D Group, IVD Business Team, Health and Medical Equipment Division, Samsung Electronics Co., Ltd., 129, Samsung-ro, Yeongtong-gu, Suwon-si, Gyeonggi-do, Republic of Korea. E-mail: sh8665.park@samsung.com, m0855@naver.com

† Electronic supplementary information (ESI) available. See DOI: 10.1039/c9an00555b

ethanesulfonic acid, CHAPS, D-sorbitol, and glycerol were purchased from Dojindo (Kumamoto, Japan). NaOH (4 N), D-sorbitol, polyvinylbutyral (PVB), bromocresol purple (BCP), glycylglycine, citric acid, and Triton X-100 were purchased from Wako Pure Chemical Industries (Osaka, Japan). Urease (URH-201) was purchased from Toyobo (Osaka, Japan). l-γ-Glutamyl-3 carboxyl-4-nitroanilide (γ-GCN) was purchased from Roche (Basel, Switzerland). A chloride electrode, urea/blood urea nitrogen (BUN) kinetic Modular P liquid, gamma-glutamyl transpeptidase (GGT) Modular P liquid, and total bilirubin Modular P liquid were purchased from Roche Diagnostics GmbH (Mannheim, Germany). Hemoglobin reagent was purchased from Randox Laboratories (Crumlin, UK). Multiple VALIDATE kits were purchased from LGC Maine Standards (Cumberland Foreside, ME, US). All other chemicals were purchased from Sigma-Aldrich.

2.2 Reagent design for the chloride, BUN, and GGT sensors

An optode membrane and buffer mixture were prepared for the chloride sensor. The chloride optode polymeric membrane mixture was prepared from 4% (w/v) poly(vinyl chloride), 21% (v/v) bis(2-ethylhexyl)sebacate, 4% (v/v) Tris(2-ethylhexyl) phosphate, 0.8% (v/v) trioctyltin chloride, 0.15% (w/v) chromoionophore VI, and 70% (v/v) cyclohexanone. After mixing for 30 s, the mixture was incubated at room temperature for 12 h. The buffer mixture was prepared from 3.2% (w/w) D-sorbitol, 2.2% (v/v) glycerol, and 0.0024% (v/v) Triton X-100 in 800 mM citric acid buffer (pH 4.5).[13,14]

An enzyme mixture and pH indicator mixture were prepared for the BUN sensor. The enzyme mixture was prepared from urease (1600 units), 2% (w/w) D-sorbitol, 0.0025% (v/v) Triton X-100, and 0.5% (w/v) CHAPS in 1 mL of 400 mM bicine buffer (pH 8.5). An 8% (w/v) PVB solution was prepared in cyclohexanone by sonicating for 20 min and mixing for 1 min. The pH indicator mixture was prepared with 4.5% (v/v) PVB using the 8% PVB solution, 0.13% BCP, and 95% (v/v) cyclohexanone with vigorous mixing for 10 min.

A γ-GCN mixture and buffer mixture were prepared for the GGT sensor. The γ-GCN mixture was prepared from 6.25% (w/v) γ-GCN, 5% (w/w) D-sorbitol, and 0.4% (w/v) CHAPS in 10 mM 2-(*N*-morpholino)ethanesulfonic acid buffer (pH 5.5), and mixed for 30 s. The buffer mixture was prepared from 1% (w/w) D-sorbitol, 0.2% (w/v) CHAPS in 300 mM glycylglycine buffer (pH 8.0).

2.3 Construction of the sensor chips for the chloride, BUN, and GGT reagents

The sensor chip was manufactured to measure the reagents in a specific optical device (LabGEO PT10; Samsung Electronics Co., Ltd, Korea). The sensor chip consisted of two polyethylene terephthalate (PET) films, spacer sheet, and was very thin (300 μm) (Fig. S1a†).[14] The prepared reagents for the chloride, BUN, and GGT sensors were applied on the two PET films and then incubated at 1% humidity for 24 h. The thickness of the dried chloride sensor on the film was 40 μm ± 0.44, and both the dried BUN and GGT sensors were 50 μm ± 0.55 thick (Fig. S1b†). Each reagent-coated PET film was attached to a spacer sheet and laminated (Fig. S1c†). The final assembled sensor chips were evaluated using test samples in the LED-based optical device and were capable of measurements at 405 nm, 450 nm, 535 nm, 630 nm, and 810 nm (Fig. S1d†). The absorbance values for the chloride, BUN, and GGT sensors were calculated using the following equations (eqn (1)–(3)):

$$\text{Absorbance calculation for the chloride sensor} = \left[\text{OD}_{(535-810\,\text{nm})}(300\,\text{s})\ \text{in W1} - \text{OD}_{(535-810\,\text{nm})}\text{in W2}\right] / \left[\text{OD}_{(535-810\,\text{nm})}(\text{before reaction})\,\text{in W1}\right] \quad (1)$$

$$\text{Absorbance calculation for the BUN sensor} = \left[\text{OD}_{(535-810\,\text{nm})}(240\,\text{s})\,\text{in W1}\right] \quad (2)$$

$$\text{Absorbance calculation for the GGT sensor} = \left[\text{OD}_{(405-810\,\text{nm})}(300-240\,\text{s})\,\text{in W1}\right] \quad (3)$$

where W1 is the sensor reaction well, W2 is the sample measurement well, and OD is the optical density (Fig. 1).

2.4 Regression analysis

Venous blood samples were collected into heparinized tubes. The samples were centrifuged at 1000*g* for 15 min, and the plasma was retained. The chloride electrode, urea/BUN kinetic Modular P liquid, GGT Modular P liquid, total bilirubin Modular P liquid, and hemoglobin reagent with the samples were operated relative to a reference device (P-modular clinical chemistry analyzer; Roche Diagnostics GmbH) to measure the reference concentrations of chloride, GGT, BUN, bilirubin, and hemoglobin. The samples were placed in the optical device to obtain the absorbance values at 405 nm, 450 nm, 535 nm, 630 nm, and 810 nm using the sensor chips. Regression analysis was performed using SigmaPlot (version 13.0; Systat Software, Inc., San Jose, CA, US) with the absorbance values and the reference concentrations of chloride, BUN, GGT, bilirubin, and hemoglobin.

2.5 Calibration

Calibration was performed to calculate the concentrations of chloride, BUN, and GGT using the absorbance values measured by the sensor chips by the optical device. Multiple VALIDATE kits were used for calibration. The mean absorbance values of duplicate measurements from the optical device and typical reference values for each calibrator were used to calculate polynomial regression equation values, which were obtained using SigmaPlot. The calculated polynomial regression values were applied to the method comparison and interference test, which used the concentration calculated in the optical device using the calibrator.

2.6 Method comparison

A method comparison was carried out in accordance with the Clinical and Laboratory Standards Institute (CLSI) EP9-A2 guideline.[15] The chloride electrode, urea/BUN kinetic

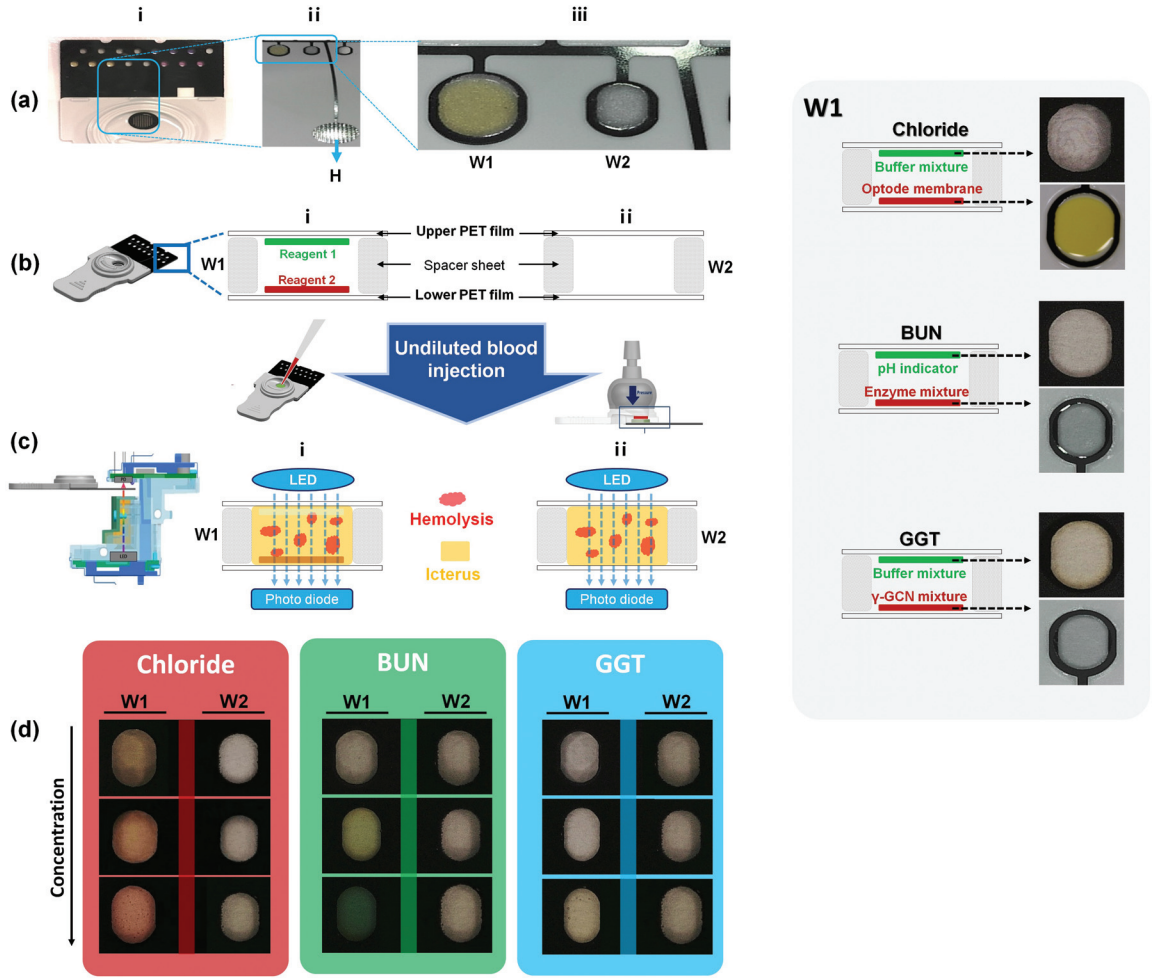

Fig. 1 Structure of the sensor chip for the chloride, BUN, and GGT sensors and optical measurements. (a) H is the sample injection hole, W1 is the sensor reaction measurement well, and W2 is the sample measurement well. (b) Side view of W1 and W2. W1 contains reagents 1 and 2 for the chloride, BUN, and GGT measurements. W2 is empty to allow for measurement of the absorbance of the blood sample itself. (c) When the undiluted blood sample containing interferents produced by hemolysis or icterus is injected on H, it is moved into W1 and W2. In W1, it reacts with the sensor. The sample in W1 and W2 is analyzed using the LED. (d) Colors in W1 and W2 before and after blood sample injection. W1 shows the color change caused by reaction of the sensor reagents and sample. W2 shows the color of the sample injected into the empty well.

Modular P liquid, GGT Modular P liquid, total bilirubin Modular P liquid, and hemoglobin reagent with the clinical samples were operated relative to the reference device to measure the reference concentrations of chloride, GGT, and BUN. The concentrations of chloride, GGT, and BUN measured by the optical device using the clinical samples were compared with the reference concentrations. Statistical comparisons were performed using Analyse-it SW (method validation edition; Analyse-it Software, Ltd, UK) for Passing–Bablok analysis, and the R Score, slope, and offset values were calculated. The observed % bias and total error were calculated (eqn (4)):

$$\%\,\text{bias}(d_{\text{obs}}\%) = \frac{\text{test} - \text{reference}}{\text{reference}} \times 100. \quad (4)$$

2.7 Interference tests

Interference tests were carried out in accordance with the CLSI EP7-A2 guideline.[16] Clinical samples with low and high concentrations of chloride (low: ≤90 mmol L^{-1}, high: ≥120 mmol L^{-1}), BUN (low: ≤20 mg dL^{-1}, high: ≥60 mg dL^{-1}), and GGT (low: ≤30 U L^{-1}, high: ≥90 U L^{-1}), as assessed on the reference device, were spiked with bilirubin (1–50 mg dL^{-1}) and hemoglobin (10–500 mg dL^{-1}). Each prepared sample was tested four times in the optical device. The interference effect rate (dobs, %) was determined using the means of the test and control as follows (eqn (5)):

$$\text{Interference effect rate}(d_{\text{obs}}\%) = \frac{\text{mean(test)} - \text{mean(control)}}{\text{mean(control)}} \times 100. \quad (5)$$

3 Results and discussion

3.1 Target analytes and reagent sensor design

To investigate the diverse interference effects caused by icterus and hemolysis of blood, it was necessary to select analytes

from different assay methods. The target analytes selected were chloride, BUN, and GGT. These analytes can be encountered with different assays and allow for investigation of a range of interference effects. Chloride is an electrolyte that can help control the volume of fluids and balance of acids and bases in the human body.[17–19] GGT is found in the liver and biliary epithelial cells, and is a sensitive marker of hepatobiliary disease.[20,21] BUN is a factor that measures the amount of urea nitrogen found in the blood.[22,23]

The analytes are detected using chemical (chloride), biochemical with a color reagent (BUN), and biochemical without a color reagent (GGT) assays. The chloride sensor design included an ionophore and chromoionophore. Trioctyltin chloride acts as an ionophore that reacts with chloride ions in the sample, which results in protonation and a conformational change of the chromoionophore. The ion concentration is determined by measuring the $OD_{(535–810\ nm)}$ (Fig. S2a†).[13] The BUN sensor design incorporated quantification of ammonia release from urea by urease catalysis. The released ammonia results in a color change of the pH indicator (BCP), which can be measured at $OD_{(535–810\ nm)}$ (Fig. S2b†).[22,24] The GGT sensor design incorporated quantitative measurement of γ-GCN without a chromogen. GGT catalyzes the transfer of the glutamyl group from γ-GCN to glycylglycine. The amount of 5-amino-2-nitrobenzoate formed is proportional to the GGT activity and can be measured at $OD_{(405–810\ nm)}$ (Fig. S2c†).[25,26]

3.2 Sensor chip composition for optical measurements

Two measurement wells were needed to investigate the interference effects caused by icterus and hemolysis in blood. The first well measured the change in the color of the sensor on reaction with the sample, and the second well measured the optical value of the unreacted sample. Fig. 1 shows the struc-

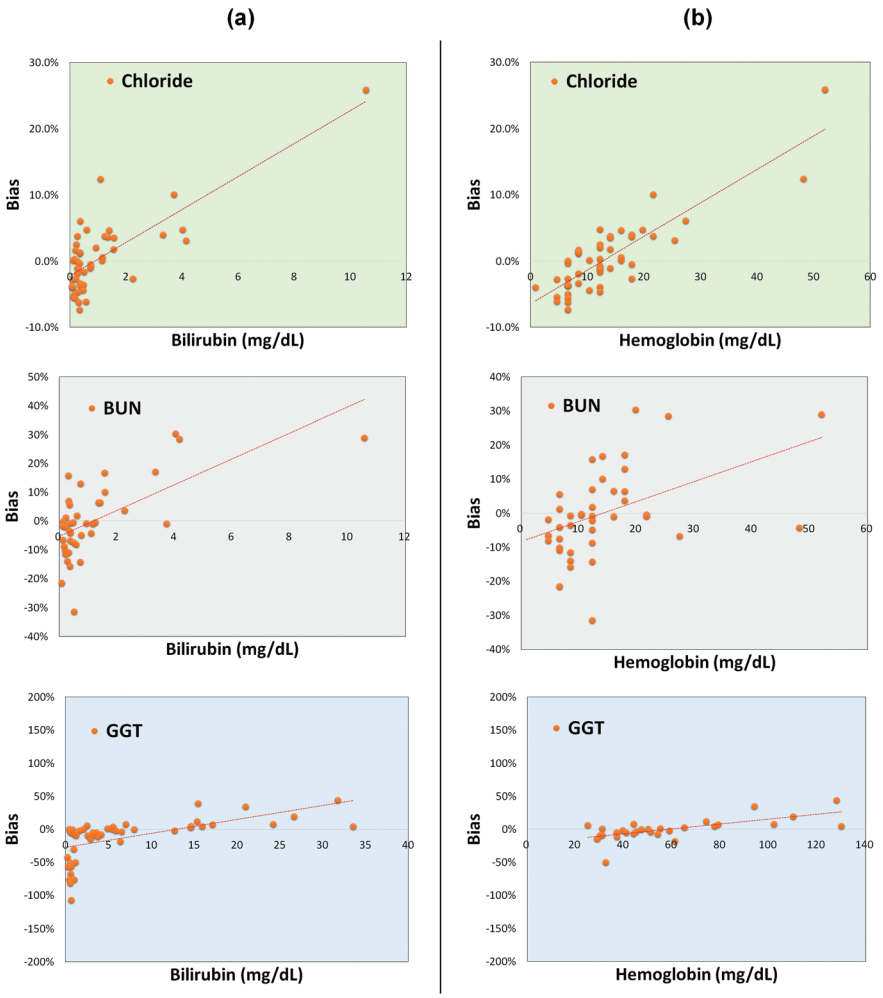

Fig. 2 Scatter plot to confirm the bias (%) trend with increasing bilirubin and hemoglobin concentrations. Undiluted clinical samples (n = 49 for chloride, n = 41 for BUN, and n = 54 for GGT) were analyzed using the chloride, BUN, and GGT sensor chips in the optical device, and the absorbance values were obtained. The absorbance values were calculated (see eqn (1)–(3)). The concentrations of chloride, BUN, and GGT were obtained by calibration using the calculated absorbance values. The clinical samples were measured in the reference device to obtain reference concentrations of chloride, GGT, BUN, bilirubin, and hemoglobin. The bias (%) between the concentrations measured in the optical device and the reference concentrations was determined from the bilirubin (a) and hemoglobin (b) concentrations (see eqn (4)).

ture of the sensor chip used for the chloride, BUN, and GGT sensors, including the exterior and interior of the measurement component, which contains the two wells and a sample injection hole. The sample hole was configured so the sample could be injected (Fig. 1ai and ii), and the injected sample was moved to the wells through a microfluidic channel (Fig. 1aiii). The sensor reaction measurement well (W1) consisted of reagent sensors on the lower and upper PET film. W1 contained the following: the optode membrane on the lower PET film and buffer mixture on the upper PET film for the chloride sensor, the enzyme mixture on the lower PET film and pH indicator on the upper PET film for the BUN sensor, and the γ-GCN mixture on the lower PET film and buffer mixture on the upper PET film for the GGT sensor (Fig. 1b). These were prepared in the solid state to evaluate the high interference effect that could arise with an undiluted sample. The sample measurement well (W2) was empty (Fig. 1bii). When a sample was injected into W1 (Fig. 1ci) and W2 (Fig. 1cii), the reaction in each well was measured using the optical device. The absorbance values measured in W1 depended on the color change of the reagent sensor, and the optical value of the sample itself was measured in W2 (Fig. 1d).

3.3 Interference effects caused by hemolysis and icterus of blood in the chloride, BUN, and GGT sensors

Interference caused by hemolysis occurs when hemoglobin is released into plasma, and interference caused by icterus occurs when samples have high bilirubin concentrations. Therefore, to investigate the effects of interference caused by icterus and hemolysis of blood on the chloride, BUN, and GGT sensors, the concentrations of chloride, GGT, BUN, bilirubin and hemoglobin in clinical samples were measured using the reference device. The results were used as reference concentrations. The same clinical samples were analyzed using the chloride, BUN, and GGT sensors without sample dilution in the optical device. The bias (%) between the concentrations measured using the sensor chips and reference device was evaluated. As the concentrations of bilirubin and hemoglobin

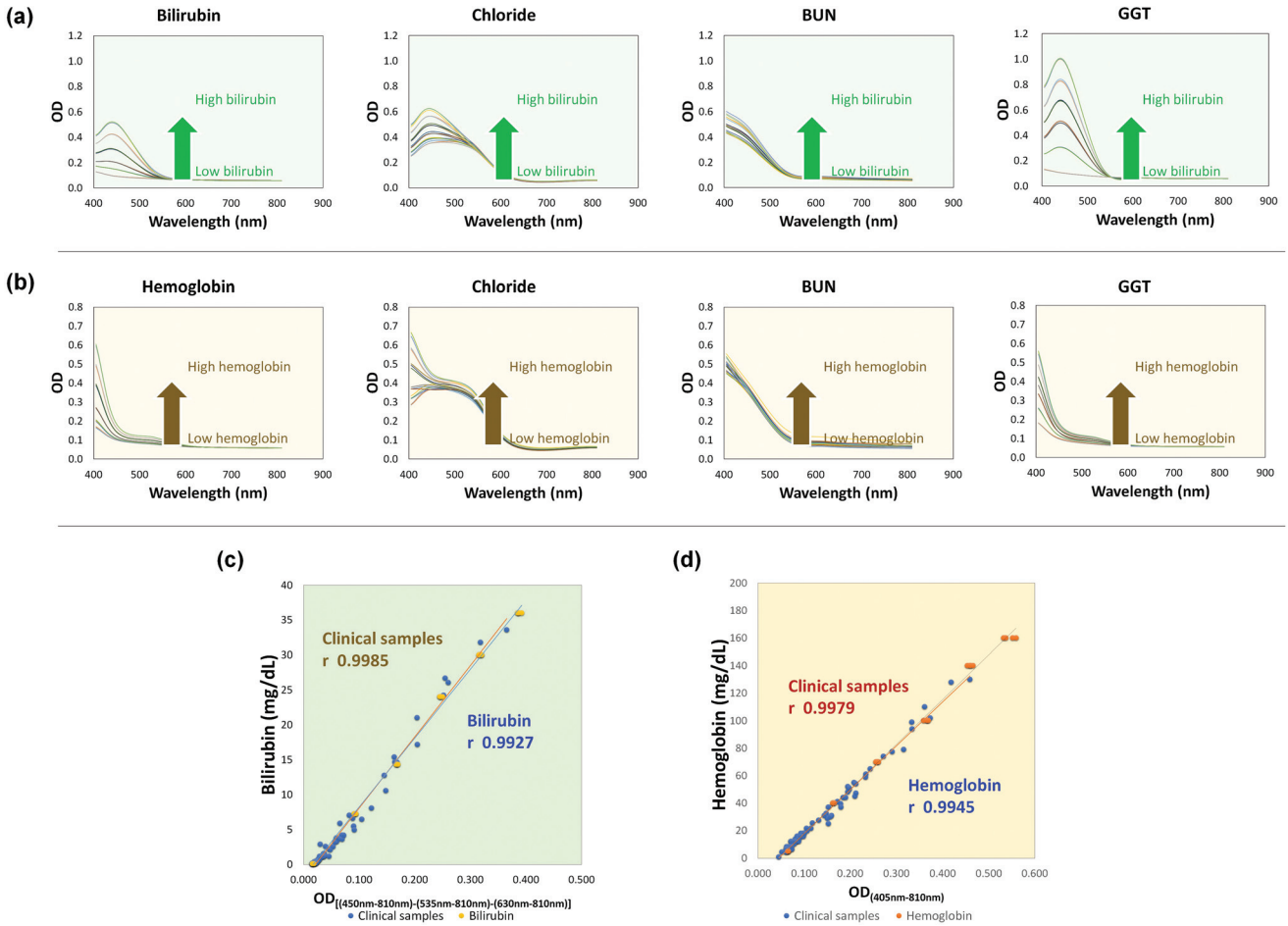

Fig. 3 Visible spectra and linear regression with increasing bilirubin and hemoglobin concentrations. (a and b) Clinical samples spiked with bilirubin and hemoglobin at six concentration levels were analyzed using the chloride, BUN, and GGT sensor chips in the optical device. Each sample was analyzed three times. The visible spectra of bilirubin and hemoglobin in (a) and (b) were measured in W2. The visible spectra of chloride, BUN, and GGT in (a) and (b) were measured in W1. (c and d) Clinical samples (n = 79) and bilirubin- and hemoglobin-spiked clinical samples (six levels × three times) measured at $OD_{(405–810\ nm)}$, $OD_{(450–810\ nm)}$, $OD_{(535–810\ nm)}$, and $OD_{(630–810\ nm)}$ by the optical device. $OD_{[(450–810\ nm)–(535–810\ nm)–(630–810\ nm)]}$ was calculated and fitted with the reference bilirubin concentration (c). $OD_{(405–810\ nm)}$ was fitted with the reference hemoglobin concentration (d).

increased, the bias (%) also increased (Fig. 2a and b). According to these results, the concentrations measured by the chloride, BUN, and GGT sensors are affected by the concentrations of bilirubin and hemoglobin.

3.4 Correlation between the bilirubin and hemoglobin concentrations and the signal absorbances of clinical samples

Clinical samples spiked with bilirubin and hemoglobin were analyzed, and the visible spectra measured in W1 and W2 were confirmed to clarify specific reactions of the sensor reagents with bilirubin and hemoglobin. The bilirubin and hemoglobin results in W2 confirmed that the absorbance increased when the concentration increased. The chloride, BUN, and GGT results measured in W1 also confirmed that the absorbance increased as the bilirubin and hemoglobin concentrations increased (Fig. 3a and b). This means that there must be a absorbance that can accurately reflect the hemoglobin and bilirubin concentrations. Therefore, a absorbance equation was developed for hemoglobin and bilirubin.

Regression analysis was performed using the bilirubin and hemoglobin concentrations measured in the reference device and the absorbance measured in W2 using the sensor chip in the optical device. The absorbance values of 79 undiluted clinical samples were measured in W2 using the sensor chip in the optical device, and each absorbance was fitted with the bilirubin and hemoglobin concentrations. The $OD_{[(450–810\ nm)–(535–810\ nm)–(630–810\ nm)]}$ showed a high correlation with the bilirubin concentration (r = 0.9985) (Fig. 3c). The $OD_{(405–810\ nm)}$ showed a high correlation with the hemoglobin concentration (r = 0.9979) (Fig. 3d). The regression curves of the clinical samples were well matched with the bilirubin- and hemoglobin-spiked samples. As shown in the screening results for other absorbance values, the correlation with clinical samples was low or the signal response curve between the clinical samples and the spiked samples did not match well (Fig. S3a–d and S4b–d†). In previous reports of hemolysis measurements, some were performed at $OD_{(600\ nm/570\ nm)}$ and one at $OD_{415\ nm}$. The results confirmed that the correlation with hemolysis was high in the $OD_{405\ nm}$ region, similar to the results in the study that used $OD_{415\ nm}$.[1,27]

3.5 Improvement in chloride, BUN, and GGT performance by deletion of the bilirubin and hemoglobin signals

The $OD_{[(450–810\ nm)–(535–810\ nm)–(630–810\ nm)]}$ showed a high correlation with the bilirubin concentration, and the $OD_{(405–810\ nm)}$ showed a high correlation with the hemoglobin concentration. The tendency of an increase in the bias (%) of chloride, BUN, and GGT was confirmed by increasing the bilirubin and hemoglobin concentrations. Therefore, the performance of the chloride, BUN, and GGT sensors may be improved by deleting the signal absorbance values for bilirubin and hemoglobin in clinical samples. The following equations were used to remove bilirubin and hemoglobin interference from the chloride, BUN, and GGT sensors (eqn (6)–(10)):

$$\mathrm{BID} = \mathrm{OD}_{[(450–810\,\mathrm{nm})–(535–810\,\mathrm{nm})–(630–810\,\mathrm{nm})]} \quad (6)$$

$$\mathrm{HID} = \mathrm{OD}_{(405–810\,\mathrm{nm})} \quad (7)$$

$$\text{Nf selection} : (\mathrm{BID} + \mathrm{HID})/C \quad (8)$$

$$\mathrm{IID} = (\mathrm{BID} + \mathrm{HID}) \times \mathrm{Nf}^{-1} \quad (9)$$

$$\text{Interference effect improved absorbance value} = C \pm \mathrm{IID} \quad (10)$$

where C is the value calculated using the absorbance measured in the sensor for the target analyte (see eqn (1)–(3)); IID is the interference index detection, which is a total index for bilirubin and hemoglobin interference detection; BID is the bilirubin index detection, which is the $OD_{[(450–810\ nm)–(535–810\ nm)–(630–810\ nm)]}$ of the sample measured in W2; HID is the hemolysis index detection, which is the $OD_{(405–810\ nm)}$ of the sample measured in W2; and Nf is a normalization factor. The BID and HID may be different because of variation in factors such as the reagent

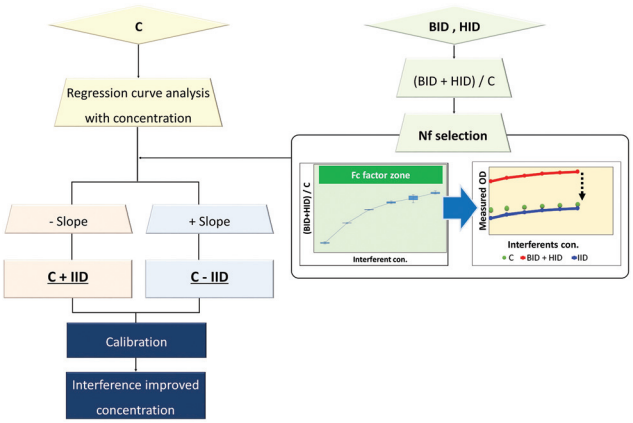

Fig. 4 Logic for interference index detection (IID) operation. BID is the bilirubin index detection, HID is the hemolysis index detection, C is the value calculated using the absorbance value measured for the sample reaction in the sensor chip (see eqn (1)–(3)), and Nf is the normalization factor.

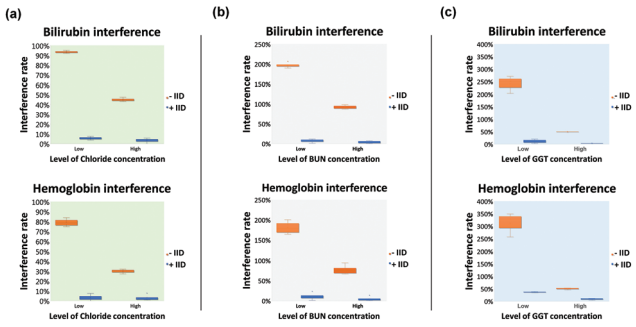

Fig. 5 Interference tests of the chloride, BUN, and GGT sensors with the IID system. Bilirubin-spiked, hemoglobin-spiked, and non-spiked clinical samples (low and high concentrations of chloride, BUN, GGT) were measured using the chloride, BUN, and GGT sensor chips in the optical device. Each sample was analyzed three times. The interference rates of the (a) chloride, (b) BUN, and (c) GGT sensors with (see eqn (10)) and without (see eqn (1)–(3)) the IID system were compared (see eqn (5)).

composition, reagent concentration, light path length, applied chromogen, and scale of the calculated absorbance values. Therefore, a factor may be required to normalize the BID and HID values.

Fig. 4 shows the logic used to remove interference effects using the optical formula. The samples were reacted to measure the absorbance values using the chloride, BUN, and GGT sensor chips, and the values of C were calculated for the target substance. The direction (±) of the slope was checked by regression analysis using the C values and interference concentrations. The chloride slope was negative (Fig. S5†), and the BUN (Fig. S6†) and GGT (Fig. S7†) slopes were positive. The absorbance values from the bilirubin and hemoglobin concentrations of the samples were measured in W2 (interfering substance). The absorbance values were calculated using BID and HID. The Nf value was selected to normalize the values of BID and HID to the value of C. The Nf value for each interference concentration was calculated using the equation (BID + HID)/C, and the Nf value selected was above the maximum concentration of the measured interference material. The Nf values for the IID of the chloride, BUN, and GGT sensors were 1, 15, and 150, respectively (Fig. S5–S7†).

If the slope was negative, the absorbance values were calculated using C + IID. If the slope positive, the absorbance values were calculated using C − IID. The absorbance values were calibrated using calibrators to obtain the concentrations.

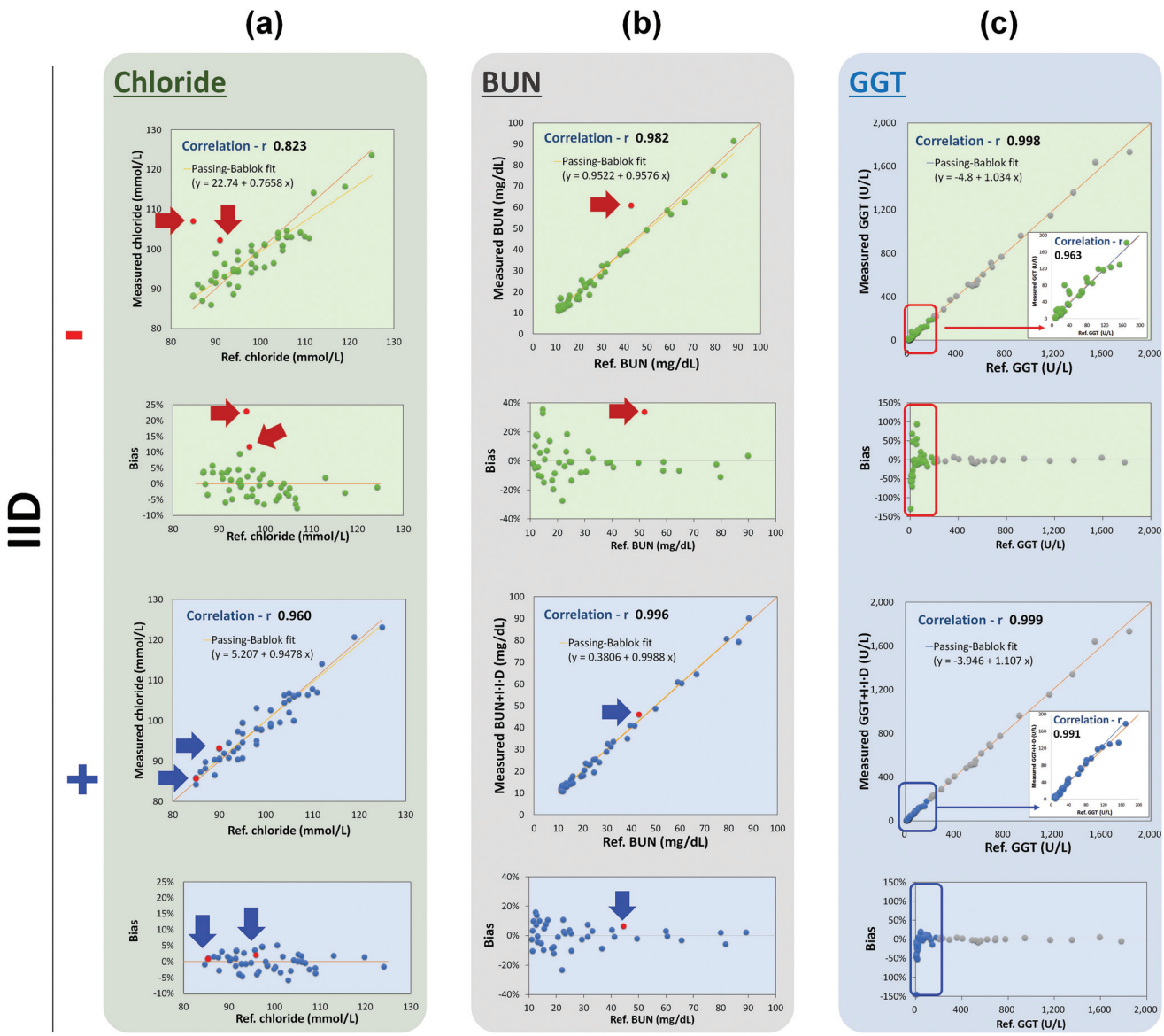

Fig. 6 Comparison of the chloride, BUN, and GGT sensors with the IID system. Undiluted clinical samples (n = 49 for chloride, n = 41 for BUN, and n = 54 for GGT) were measured using the chloride, BUN, and GGT sensor chips in the optical device. The clinical samples were also measured in the reference device to obtain reference concentrations of chloride, GGT, and BUN. The (a) chloride, (b) BUN, and (c) GGT concentrations from the optical device (with (see eqn (10)) and without (see eqn (1)–(3)) the IID system) and the reference device were compared. Passing–Bablok and Bland–Altman difference plot analyses with 95% CI were performed to confirm the R score, slope, offset, and % bias (see eqn (4)).

3.6 Interference test for verification of the IID system

Interference tests were performed to verify the clinical performance of the IID system as shown in Fig. 4. The tests were carried out using clinical samples spiked with hemoglobin (~500 mg dL^{-1}) and bilirubin (~50 mg dL^{-1}). The bilirubin interference rates (mean) with the chloride sensor and the IID system decreased from 93% to 6% (low chloride) and 45% to 3% (high chloride), and the hemoglobin interference rates (mean) decreased from 79% to 3% (low chloride) and 30% to 3% (high chloride) (Fig. 5a and S8†). The bilirubin interference rates (mean) with the BUN sensor and the IID system decreased from 197% to 7% (low BUN) and 93% to 4% (high BUN), and hemoglobin interference rates (mean) decreased from 181% to 11% (low BUN) and 77% to 5% (high BUN) (Fig. 5b and S9†). The bilirubin interference rates (mean) with the GGT and the IID system decreased from 243% to 12% (low GGT) and 50% to 4% (high GGT), and the hemoglobin interference rates (mean) decreased from 312% to 37% (low GGT) and 51% to 9% (high GGT), respectively (Fig. 5c and S10†).

3.7 Method comparison for verification of the IID system

The IID system reduced hemoglobin and bilirubin interference. A method comparison test was performed to confirm the correlation performance of the clinical samples with the interference effect improvement. The reference concentrations of chloride, BUN, GGT, bilirubin, and hemoglobin for the clinical serum samples were obtained using the reference device. The undiluted clinical samples were analyzed using the chloride, BUN, and GGT sensors, and the concentrations calculated using the IID applied absorbance value were compared with the reference concentrations. The IID had a positive effect on reducing interference with the chloride, BUN, and GGT sensors and improving the accuracy of the clinical sample results. A scatter plot was used to analyze the bias (%) according to the bilirubin and hemoglobin concentrations. Before applying the IID, the bias (%) increased as the bilirubin and hemoglobin concentrations increased. However, after applying the IID, the bias (%) improved (Fig. S11a and b†). The method comparison using clinical samples showed that the correlations (R) of the chloride, BUN, and GGT sensors improved from 0.823 to 0.960, 0.982 to 0.996, and 0.998 to 0.999, respectively, after applying the IID and the bias (%) results for individual sample measurements were significantly improved (Fig. 6). The IID effectively reduces the effect of interference with the chloride and BUN sensors (red and blue arrows in Fig. 6a and b). In the GGT sensor, the clinically important concentration range of GGT is near the reference range (0–200 U L^{-1}), and was particularly improved (red and blue boxes in Fig. 6c). Therefore, the IID removed bilirubin and hemoglobin interference, and improved the correlation.

4 Conclusions

An IID system was developed to improve the measurement accuracy of chemical sensors used in clinical applications by removing the optical characteristics of interference caused by icterus and hemolysis in blood samples. The sensor accuracy was analyzed using data from real clinical samples, and interference tests and a method comparison using CLSI guidelines were conducted to increase the reliability of the validation procedure. The IID used optical measurements of clinical blood samples to minimize the interference effect.

Diagnostic assays of blood utilize various sensors, such as chemical, enzymatic, and optode, according to the characteristics of the target analytes. Interferents will differ depending on the assay method and reagents. Therefore, three different assay methods were investigated in this study: chemical, biochemical using a color reagent, and biochemical without a color reagent. The results were used to evaluate the use of the IID in different assays. The IID effectively reduced interference from high concentrations of bilirubin and hemoglobin, and improved the measurement accuracy. Therefore, the IID is expected to be useful in IVD devices. Further studies could improve the interference effect through optimization of the optical algorithm for other analytes and biosensors.

Generally, most bioassays require sample dilution with a liquid reagent to avoid interference. This additional step for sample preparation negatively impacts the assay usability and increases the measurement time. The IID system efficiently reduces interference even in undiluted clinical samples. In addition, the IID system can be easily applied with only two wells and an optical component. Therefore, the IID system will simplify bioassays.

Ethical approval

All experiments were performed in accordance with the IRB Guidelines, and approved by the ethics committee at Kangbuk Samsung Hospital (KBSMC2016-01-012). Informed consents were obtained from human participants of this study.

Conflicts of interest

Author has no conflicts of interest with the published study.

Acknowledgements

This study was supported by Health and Medical Equipment Division of Samsung Electronics under Project Number RAU0118ZZ-01MZ.

References

1 C. J. L. Farrell and A. C. Carter, *Ann. Clin. Biochem.*, 2016, **53**, 527–538.
2 Clinical and Laboratory Standards Institute, C56, 2011.
3 P. Carraro, G. Servidio and M. Plebani, *Clin. Chem.*, 2000, **46**, 306–307.

4 W. G. Guder, *J. Clin. Chem. Clin. Biochem.*, 1986, **24**, 125–126.
5 G. Lippi, N. Blanckaert, P. Bonini, S. Green, S. Kitchen, V. Palicka, A. J. Vassault and M. Plebani, *Clin. Chem. Lab. Med.*, 2008, **46**, 764–772.
6 E. J. McCaughey, E. Vecellio, R. Lake, L. Li, L. Burnett, D. Chesher, S. Braye, M. Mackay, S. Gay, T. Badrick, J. Westbrook and A. Georgiou, *Crit. Rev. Clin. Lab. Sci.*, 2017, **54**, 59–72.
7 P. K. Nigam, *Indian J. Clin. Biochem.*, 2016, **31**, 237–239.
8 L. Sciacovelli, A. Aita, A. Padoan, M. Pelloso, G. Antonelli, E. Piva, M. L. Chiozza and M. Plebani, *Clin. Chem. Lab. Med.*, 2016, **54**, 1169–1176.
9 G. Lippi, G. L. Salvagno, M. Montagnana, G. Brocco and G. C. Guidi, *Clin. Chem. Lab. Med.*, 2006, **44**, 311–316.
10 N. Nara, N. Andrade, M. V. Oliveira and C. L. Souza, *J Bras Patol Med Lab*, 2016, **52**, 103–106.
11 E. Fliser, K. Jerkovič, T. Vidovič and M. Gorenjak, *Biochem. Med.*, 2012, **22**, 352–362.
12 N. Nikolac, *Biochem. Med.*, 2014, **24**, 57–67.
13 S. S. S. Tan, P. C. Hauser, K. Wang, K. Fluri, K. Seiler, B. Rusterholz, G. Suter, M. Krüttli, U. E. Spichiger and W. Simon, *Anal. Chim. Acta*, 1991, **255**, 35–44.
14 J. Lee, Y. K. Hahn, J.-Y. Park, H. Seo, J. Jung, E. Cho, Y.-S. Choi and S. S. Lee, *Sens. Actuators, B*, 2019, **280**, 256–262.
15 CLSI, *Method Comparison and Bias Estimation Using Patient. Samples; Approved Guideline – Second Edition (Interim Revision) CLSI Document EP09-A2-IR*, Clin. Lab. Stand. Inst., Wayne, PA, 2010.
16 Clinical and Laboratory Standards Institute, *Interference Testing in Clinical Chemistry; Approved Guideline—Second Edition*, 2005.
17 D. MacClelland, *AORN J.*, 1975, **21**, 1146.
18 P. E. Mullis, P. C. Hindmarsh and C. G. D. Brook, *Eur. J. Pediatr.*, 1990, **150**, 22–25.
19 S. Vallejos, E. Hernando, M. Trigo, F. C. García, M. García-Valverde, D. Iturbe, M. J. Cabero, R. Quesada and J. M. García, *J. Mater. Chem. B*, 2018, **6**, 3735–3741.
20 J. H. D. A. van Beek, M. H. M. de Moor, E. J. C. de Geus, G. H. Lubke, J. M. Vink, G. Willemsen and D. I. Boomsma, *Behav. Genet.*, 2013, **43**, 329–339.
21 J. B. Whitfield, *Crit. Rev. Clin. Lab. Sci.*, 2001, **38**, 263–355.
22 J. A. Kruse, *JAMA, J. Am. Med. Assoc.*, 1990, **264**, 2808.
23 C. J. Percival, S. Stanley, A. Braithwaite, M. I. Newton and G. McHale, *Analyst*, 2002, **127**, 1024–1026.
24 Y. L. Lin, C. T. Chen, S. C. Lin, C. Lee, H. S. Kuo, C. M. Shih, Y. H. Hsu, Y. P. Chin and E. C. Chan, *Biotechnol. Lett.*, 2000, **9**, 249–255.
25 C. A. Burtis, E. R. Ashwood and D. E. Bruns, *Tietz Fundamentals of Clinical Chemistry*, 2008.
26 F. Caravaca-Fontán, L. Azevedo, M. Á. Bayo, B. Gonzales-Candia, E. Luna and F. Caravaca, *Nefrologia*, 2017, **37**, 267–275.
27 G. Lippi, J. Cadamuro, E. Danese, M. Gelati, M. Montagnana, A. von Meyer, G. L. Salvagno and A.-M. Simundic, *PLoS One*, 2018, **13**, e0200088.